

RESEARCH ARTICLE**Contrasting pre-vaccine COVID-19 waves in Italy through Functional Data Analysis**Tobia Boschi^{†1} | Jacopo Di Iorio^{†2} | Lorenzo Testa^{†3} | Marzia A. Cremona^{*4,5} | Francesca Chiaromonte^{*2,3}¹IBM Research Europe, Dublin, Ireland²Department of Statistics, Penn State University, University Park, Pennsylvania (US)³L'EMbeDS, Sant'Anna School of Advanced Studies, Pisa, Italy⁴Department of Operations and Decision Systems, Université Laval, Québec, Canada⁵CHU de Québec – Université Laval Research Center, Québec, Canada**Correspondence**^{*}Marzia A. Cremona (marzia.cremona@fsa.ulaval.ca); Francesca Chiaromonte (fxc11@psu.edu)**Summary**

We use data from 107 Italian provinces to characterize and compare mortality patterns in the first two COVID-19 epidemic waves, which occurred prior to the introduction of vaccines. We also associate these patterns with mobility, timing of government restrictions, and socio-demographic, infrastructural, and environmental covariates. Notwithstanding limitations in accuracy and reliability of publicly available data, we are able to exploit information in curves and shapes through Functional Data Analysis techniques. Specifically, we document differences in magnitude and variability between the two waves; while both were characterized by a co-occurrence of “exponential” and “mild” mortality patterns, the second spread much more broadly and asynchronously through the country. Moreover, we find evidence of a significant positive association between local mobility and mortality in both epidemic waves, and corroborate the effectiveness of timely restrictions in curbing mortality. The techniques we describe could capture additional signals of interest if applied, for instance, to data on cases and positivity rates. However, we show that the quality of such data, at least in the case of Italian provinces, was too poor to support meaningful analyses.

KEYWORDS:

COVID-19, Italy, Functional Data Analysis, Curve Clustering, Functional Regression, Feature Selection

1 | INTRODUCTION

On January 30, 2020, Italy recorded the first two cases of SARS-Cov-2; a couple of Chinese tourists visiting Rome. The first non-travel related case was recorded in the municipality of Codogno (Lombardia) on February 19, 2020. With outbreaks quickly emerging in Lombardia and Veneto, local lockdowns were imposed in ten municipalities in the province of Lodi, and in one municipality in the province of Padova – affecting a total of over 50,000 people. As cases and deaths mounted, local and central authorities took progressively more stringent measures to limit mobility and social gatherings, e.g., suspending university activities, educational trips, sporting events, and exhibitions. These restrictions culminated with a general nationwide lockdown (March 9, 2020) and the suspension of all non-essential production activities (March 23, 2020), and were not lifted until May – when free movement was restored within the whole national territory.

After a fairly quiet summer, many countries in Europe, including Italy, witnessed a new rise in COVID-19 cases and deaths, leading to new containment measures. Face masks became mandatory, and gathering places such as gyms, theaters, and cinemas

[†] These authors contributed equally

closed again. On November 4, 2020, in order to control the spread of the epidemic, the Italian government created a classification system whereby regions could be labeled as yellow, orange, or red based on a number of indicators of epidemic spread and stress on the healthcare infrastructure. Each color corresponded to different curfew rules and limitations on mobility. As a precautionary measure, during the holidays red-zone rules were imposed in all regions – including those where the epidemic was not raging at the time (these were the strictest rules, equivalent to the lockdown of the first wave). In January 2021, as the second wave started to subside, restrictions were loosened again to the pre-holiday color system.

Prior analyses by our group, which employed Functional Data Analysis (FDA) tools^{1,2} on data from the first COVID-19 wave at the resolution of regions, characterized different epidemic patterns unfolding in different areas of the country, and suggested a relevant role for mobility and some socio-demographic, infrastructural and environmental factors as statistical predictors of mortality³. Our results were consistent with those of many other studies^{4,5,6,7}. In this article, we analyze data from both the first and the second wave of the epidemic – focusing on the two 150-day intervals from February 25, 2020, to July 23, 2020, and from October 1, 2020, to February 27, 2021. We also increase spatial resolution considering 107 Italian provinces, as opposed to the 20 Italian regions we considered in our prior study³. This ought to prevent dilution of signals due to aggregation, and allow for a more detailed characterization of the epidemic and its associations to potential predictors – in particular, it allows us to employ more complex statistical models without overfitting⁸. Crucially, while very different in terms of restrictions regimes imposed on the population and of its mobility behaviors, the first and second waves of COVID-19 in Italy were both pre-vaccines (the vaccination campaign in the European Union, including Italy, started – for healthcare professionals and selected fragile categories – on December 27, 2020). Thus, contrasting them offers an opportunity to refine our understanding of the roles of restrictions and mobility – without having to account for the effects of the subsequent vaccination campaigns.

At the outset of our analyses, and yet among our key findings, is evidence of poor data quality. Specifically, we observe vast under-counting of deaths in the official reports, especially during the first epidemic wave^{9,10}, and alarming discrepancies in case counts. Ignoring information on cases, properly processing information on deaths, and using FDA tools, we find marked differences between the two waves. The first was more dramatic, more concentrated spatially – hitting particularly hard in a handful of provinces in Lombardia, and with relatively homogeneous timing across such provinces. In contrast, the second wave was less dramatic but more widespread – affecting more locations with less homogeneity in timing. Notably, provinces hardest hit during the first wave were among the least affected during the second; the contrast is particularly striking in the case of Bergamo, which experienced the heaviest mortality during the first wave, making headlines around the world^{11,12}, and the lightest during the second. This may be due to the fact that inhabitants of provinces hardest hit during the first wave adhered more diligently to restrictions and safety mandates during the second, to a reduced number of people at risk (as an effect of the large number of deaths among the most vulnerable individuals during the first wave), or possibly to some kind of herd immunity (as an effect of the large number of cases during the first wave)^{13,14,15}.

To evaluate how the timing of restrictions may affect epidemic unfolding, and more specifically whether introducing restrictions early enough may help curb mortality, we create an *ad-hoc* variable measuring, for each province and separately for the two waves, the area under the mortality curve up to the point in time when restrictions were imposed. Such cumulative mortality should capture how long and how much the epidemic had a chance to “build up” in the province prior to the implementation of restrictive measures. In our analyses, this variable is far stronger than socio-demographic, infrastructural, and environmental factors as a predictor of the mortality unfolding henceforth – a result consistent with findings in other recent studies^{16,17}. Assessing and comparing the role of mobility during the two waves is less straightforward. Restriction policies were very different in the two waves (uniform across the country in the first, localized and linked to the evolution of epidemic and stress parameters in the second), and so were the behaviors of the population in response to them. Likely as a consequence of these differences, the variability observed within the mobility curves of any given province, as well as the variability observed across such curves, changed markedly between the two waves. Notwithstanding these changes, we detect a strong and significant positive association between mortality and mobility in both waves – highlighting the importance of restrictions imposed specifically on the latter as tools to control the epidemic.

The remainder of the article is organized as follows. Section 2 describes data, sources, and preprocessing procedures. Section 3 presents our main results. First, we show mismatches in case and death counts across different sources and geographical resolutions. Next, we characterize mortality patterns during the two waves and evaluate the effects of various potential predictors – including socio-demographic, infrastructural, and environmental factors. Last, we study mobility curves, their dynamics, and their association with mortality curves during the two waves. Section 4 provides concluding remarks.

2 | DATA AND PREPROCESSING

2.1 | Data on deaths and cases

Unlike our previous work³, where we analyzed Italian COVID-19 mortality at the spatial resolution of regions, here we target the higher resolution of provinces. However, to date, data on COVID-19 deaths by province are still not provided by the Italian authorities. We therefore need to resort to *differential mortality*, which can be computed using the daily all-cause death counts provided by the Italian National Statistical Institute (ISTAT) for 7270 Italian municipalities (comprising about 93.5% of the Italian population). In particular, we compute differential mortality as the difference between daily deaths and the average daily deaths in the five years prior to the pandemic (2015–2019), divided by the total population as of January 1, 2019. We compute this differential mortality for each province and for each day in the first and the second waves of the epidemic – in particular in the two 150-day intervals from February 25, 2020, to July 23, 2020, and from October 1, 2020, to February 27, 2021, respectively.

Province-level differential mortality data are smoothed into curves using cubic *smoothing B-splines* with knots approximately at each week (21 knots equally spaced over 150 days – the time domain of each wave) and a roughness penalty on the curve second derivative². Employing one knot per week allows us to focus on general trends and smooth out daily fluctuations. Separately for each wave, the smoothing parameter is selected as to minimize the average generalized cross-validation (GCV) error¹⁸ across all 107 province-level curves (the same criterion is employed to smooth the other functional data sets in this study; see below). We then align the differential mortality curves using landmark registration². Specifically, for each wave, we shift curves horizontally in order to align their peaks. For curves with multiple peaks, we consider the highest peak occurring between day 10 and day 100. The new common peak time is set to be equal to the time of the earliest peak, specifically day 20 (peak of the province of Lodi) for the first wave, and day 33 (peak of the province of Cagliari) for the second wave. Finally, we add (remove) days at the end (beginning) of the domain for the shifted curves, to guarantee the same 150-day length for all curves (curves are smoothed again after this “domain integration” – choosing the smoothing parameter by minimizing the GCV criterion). As a result, the common time in each wave is the one of the province with the earliest peak. All computations are performed using the R package `fd`¹⁹.

We repeat mortality calculations at the level of regions, in order to compare results with the data provided by the Italian Civil Protection agency (Dipartimento della Protezione Civile; DPC), which releases regional daily counts of recorded COVID-19 deaths since February 2020. We divide both ISTAT differential death counts and DPC death counts by the total population as of January 1, 2019, to obtain ISTAT differential mortality and DPC mortality, respectively. We do not perform any further preprocessing, since we employ these data only for validation purposes. DPC also provides official daily counts of COVID-19 cases since February 2020 – both at the resolutions of provinces²⁰ and regions²¹. However, DPC cases data present several inconsistencies (see Section 3.1), hence we do not employ them for further analyses.

2.2 | Socio-demographic, infrastructural, and environmental data

To investigate connections between the unfolding epidemic and socio-demographic, infrastructural, and environmental factors, we focus on six scalar covariates that can be retrieved from public sources at the resolution of provinces with reasonable data quality (see Table 1). Each covariate works as a proxy for a potentially relevant factor, namely: aging of the population (`% Over 65`); quality of distributed primary health care (`Adults per family doctors`), which has been contrasted to that of centralized, hospital-based care; the potential of hospitals (`Ave. beds per hospital`), schools (`Ave. students per classroom`) and workplaces (`Ave. employees per firm`) to act as contagion hubs; and pollution levels (PM10). The significance of this kind of proxies has been shown in recent studies related to COVID-19, both focusing on the first wave of the Italian epidemic^{3,16}, and on inter-generational relationships using data from 24 countries²². In particular, the variable `% Over 65` is retrieved from ISTAT²³ at provincial level. To compute `Adults per family doctor`, we divide the population of the province as of January 2019 (from ISTAT) by the number of family doctors in the province²⁴. The latter is obtained by summing the number of family doctors at the level of “Aziende Sanitarie Locali” (Local Health Agencies, ASL) provided by the Ministry of Health for the year 2018. We manually retrieved data missing for some provinces in Lombardia, Molise, Sardegna, and Toscana from the corresponding ASL websites. To compute `Ave. beds per hospital` we use data from the Ministry of Health²⁵, which provides the number of beds per ward in each hospital in 2019. We first aggregate them over wards belonging to the same hospital, and then average over hospitals in each province. To compute `Ave. students per classroom` we use data from the Ministry of Education²⁶, which provides the number of students in each classroom of each school in the country (public or private, at every level of education), for the academic year 2019/2020. We average them over schools in each province. Missing data for Trento,

Table 1 Scalar covariates: six variables considered as proxies of potentially relevant socio-demographic, infrastructural, and environmental factors.

Covariate	Description	Year and Source
% Over 65	Aging of the population	2020, ISTAT
Adults per family doctor	Quality of distributed primary health care	2019, Ministry of Health
Ave. beds per hospital	Ability of hospitals to act as contagion hubs	2019, Ministry of Health
Ave. students per classroom	Ability of schools to act as contagion hubs	2019, Ministry of Education
Ave. employees per firm	Ability of work places to act as contagion hubs	2018, ISTAT
PM10	Pollution levels (particulates)	2019, ISTAT

Bolzano, and Aosta are filled through random forests imputation²⁷, with default parameters `maxiter=10` (maximum number of iterations performed if the stopping criterion is not met) and `ntree=100` (number of trees grown in each forest). To compute Ave. employees per firm we use data from ISTAT²⁴, which provides the number of employees per firm at the level of municipalities. We average them over firms in each province. To compute PM10 we use data from ISTAT²⁸ – which provides the average annual concentrations of PM10 (in $\mu\text{g}/\text{m}^3$) detected by air quality meters distributed over the Italian territory – and we averaged them over meters located in each province.

2.3 | Data on local mobility

We use data on daily differential mobility provided by Google at the resolution of Italian provinces²⁹. These measure the fractional reduction of mobility with respect to levels registered in the first five weeks of 2020 (January 3 to February 6), and are organized in categories based on mobility aims. Specifically, we focus on two categories that capture the local, short-range mobility of individuals, which was allowed in all provinces also during mobility restrictions: “Grocery & Pharmacy”, which accounts for local trips to grocery and pharmacy stores, and “Workplace”, which accounts for trips to workplaces. We obtain mobility curves by smoothing these daily data with the same procedure used for mortality curves (see Section 2.1).

3 | RESULTS

3.1 | Inconsistencies in death and case data

We compare data from different sources to provide insight into their quality. Specifically, the comparison of ISTAT differential mortality and DPC COVID-19 mortality at the resolution of regions reveals a vast under-counting in the DPC official reports – markedly in the first wave, but also in the second^{9,10,30} (see Figure 1A; for each region, we contrast totals over the 150 days comprised in each wave). Overall, DPC and ISTAT data become more consistent in the second wave, especially in regions such as Emilia Romagna, Lazio, Lombardia, Veneto, and Friuli Venezia Giulia. This, by and large, suggests an improvement in the official DPC COVID-19 death records – even though they remain much lower than ISTAT differential mortality in regions such as Basilicata, Calabria, and Sardegna. Notably, in Emilia Romagna and Lazio DPC records were slightly higher than ISTAT differential mortality during the second wave. This may be a consequence of the fact that the latter reflects also phenomena indirectly related to COVID-19 – affecting mortality in both directions; e.g., increases in mortality due to untreated emergencies or untimely treatment of chronic ailments, but also reductions in mortality due to fewer accidents during lockdowns or curfews.

The number of cases reported by the DPC at the two resolutions of provinces and regions harbor massive and concerning inconsistencies. As shown in Fig. 1B, by aggregating reported province-level cases into regional case counts, we obtain totals that do not match reported region-level cases. This is strikingly demonstrated by Molise and Sicilia, where the sum of the cases reported in the provinces are, respectively, over 12 and around 7 fold higher than the cases reported at regional level. Because of the vast discrepancies between provincial and regional case counts, we decided not to consider these data in our analyses.

In short, due to the strong limitations that still exist in the official COVID-19 data, we focus on mortality alone (not cases) to characterize the epidemic, and we do so using a proxy such as differential mortality (not official records) – which has its own limitations. This may indeed comprise some deaths not related, or indirectly related, to COVID-19 – but it is still more

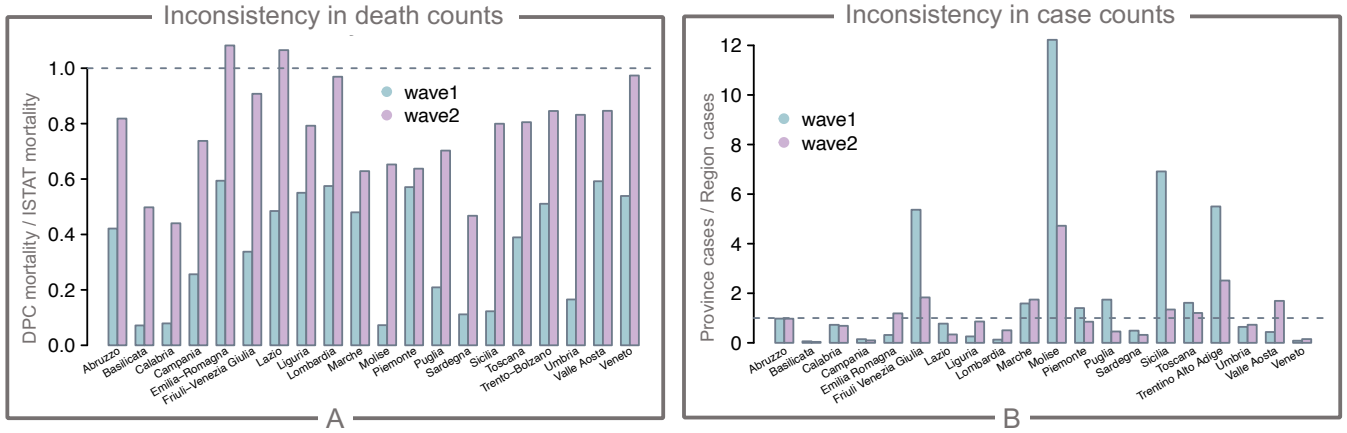


Figure 1 Inconsistencies in death and case counts. Panel A displays, for each region and wave, the ratio between COVID-19 mortality as reported by the DPC and differential mortality based on ISTAT data. During the first wave, all regions show marked inconsistencies between the two sources, suggesting a vast undercounting of deaths in the official records (ratios much lower than 1). The situation improves during the second wave; even though some regions appear to still under-report deaths (e.g., Basilicata, Calabria, Sardegna). The ratios slightly above 1 in Emilia Romagna and Lazio may reflect reductions in mortality, perhaps indirectly related to COVID-19 (e.g., fewer accidents during lockdowns and curfews), exceeding the epidemic death toll. Panel B displays, for each region and wave, the ratio between DPC case counts obtained by aggregating province-level counts within each region, and DPC case counts provided at the regional level. The inconsistencies (i.e. departures from 1) are staggering, especially during the first wave – when aggregated provincial records exceeded regional records by over 12-fold in Molise, and around 7-fold in Sicilia. As for death counts, the situation improves during the second wave, but inconsistencies remain strong enough to suggest that case count data are not to be relied on.

likely to accurately reflect mortality than the officially released deaths records, and it allows us to perform analyses at the spatial resolution of provinces.

3.2 | Mortality patterns

Our analyses, consistent with prior studies^{31,32}, delineate a dramatic and concentrated first epidemic wave – with similar timing across a small number of very hard-hit provinces, especially in Lombardia³³. In contrast, the second wave was more “spread”, with smaller differences across provinces and weaker synchronization of the mortality curves.

Fig. 2A shows aligned mortality curves during the first and second wave (see also Fig. S1 which, in addition, shows the curves before the shifts applied to align their peaks, as well as the shift distributions). Notably, the largest mortality peaks were much higher in the first wave (around 20 daily deaths per 100,000 inhabitants) than in the second (around 5 daily deaths per 100,000 inhabitants), highlighting the grim death toll Italy withstood during the former. However, such death toll was very concentrated; many curves remained low, and just a handful had very high peaks. In contrast, the mortality peaks of the second wave were less differentiated, indicating an epidemic more evenly spread across the country. In terms of timing, the first epidemic wave was markedly more synchronous than the second; this can be appreciated considering the shifts required to align peaks, which are larger (a median of 19 vs. 12 days) and more variable in the second wave (see Fig. S1).

We employ clustering techniques to characterize mortality patterns systematically, and further highlight differences in the unfolding of the two epidemic waves. We group shifted mortality curves in the first and (separately) the second wave using an agglomerative hierarchical clustering algorithm with L^2 (i.e. Euclidean) distance and complete linkage. In more detail, the L^2 distance between two generic curves x and v in the interval $[0, c]$ is defined as

$$d(x, v) = \frac{1}{c} \int_0^c (x(t) - v(t))^2 dt. \quad (1)$$

Starting from the matrix of pairwise distances, the agglomerative algorithm merges individual curves based on their distance, and clusters of curves based on the maximal distance between their members. The resulting dendrograms, one for each wave,

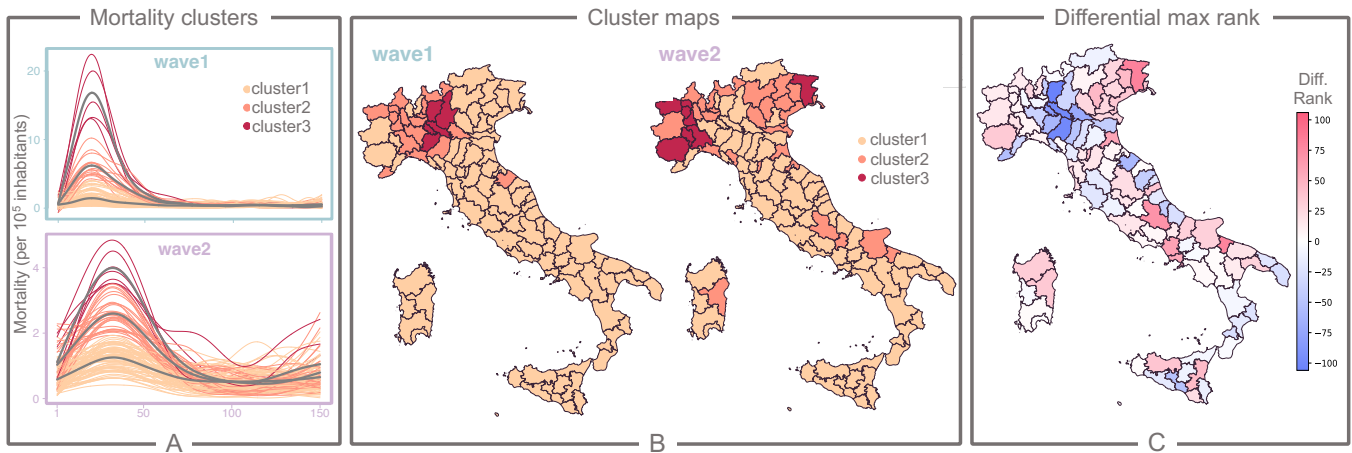


Figure 2 Clustering of mortality curves. Panel A shows aligned province-level mortality curves in the first (top) and second (bottom) waves of the epidemic. For each wave, the curves are color-coded according to a partition in three clusters – with dark red, orange, and yellow representing decreasing aggressiveness of the epidemic. Thicker gray lines trace the means of the three clusters. Panel B shows the three clusters on the Italian map, for the first (left) and second (right) wave. Panel C shows again the Italian map, with provinces color-coded based on the difference in the ranks a province occupied in the first and second wave – for each wave, we constructed rankings based on the magnitude of the curves’ largest peaks. Thus, shades of blue (red) indicate provinces that suffered the first (second) wave more than the second (first).

are shown in Fig. S2. These are cut to obtain $k = 3$ clusters in each wave, based on the dendrogram structure and the Hartigan index³⁴. The province-level aligned mortality curves in Fig. 2A are color-coded based on $k = 3$ clusters in each wave, and Fig. 2B shows the same clusters on the Italian map (cluster memberships for all provinces are reported in Fig. S3). As documented by prior studies performed at the regional level³, in the first wave Italy saw the unfolding of two very different epidemic patterns: a relatively mild one in the majority of the country, and a very strong one affecting the north-western areas. The current analysis, performed at the higher resolution of provinces, affords a more detailed description of this phenomenon: while the epidemic was more severe and more spatially concentrated in the first wave than in the second, both waves harbored two, possibly three different patterns; namely, a flatter, “mild” pattern in the majority of the provinces, a very steep, “exponential” one in a small number of provinces, and an intermediate, still “exponential” but less extreme pattern in the rest of the country.

In more detail, the provinces that withstood the most dramatic losses during the first wave were Bergamo, Brescia, Cremona, Lodi, and Piacenza. These provinces (in red in Figs. 2A and 2B) are all contiguous, in an area between Lombardia and adjacent Emilia Romagna (the very first cases of COVID-19 in the country were reported in Codogno, a municipality in the province of Lodi). Interestingly, in the second wave, all these provinces belong to the cluster with the lightest mortality (in yellow in Figs. 2A and 2B). This could be due to several factors. The inhabitants of these areas may have been more diligent in practicing social distancing rules and adhering to restrictions and safety mandates after the dramatic events of the first wave. In addition, the large number of deaths among vulnerable individuals during the first wave may have effectively reduced the number of people at risk in these areas. Finally, the large number of cases during the first wave may have induced some degree of herd immunity³⁵. In the second wave, the hardest hit provinces were Alessandria, Aosta, Asti, Biella, Cuneo, Udine, and Vercelli. Interestingly, the mortality curves for all these provinces but Vercelli are also characterized by a very large “shoulder”. The change in hardest-hit provinces with respect to the first wave, along with the fact that fewer provinces belonged to the lightest mortality cluster (in the first wave the yellow, orange, and red clusters, from lightest to hardest hit, comprised 86, 16 and 5 provinces, respectively; these counts for the second wave were 72, 28 and 7), confirm that, while less severe in terms of mortality, the epidemic had a broader spread across the country in the second wave.

We further compare the two waves considering the ranking of the provincial level mortality curves based on their peaks (maxima; from smallest to largest) and the differences between such rankings – specifically, ranking in the second wave minus ranking in the first. These differences are color-coded on the Italian map of Fig. 2C, and show very clearly how many among the provinces most affected in the first wave (highest ranks) were among the least affected in the second (lowest ranks). The

province of Bergamo is the clearest example; it ranked 107th in the first wave and 1st in the second. In contrast, some provinces in Piemonte were hard hit (high ranks) in both first and second waves – showing very little difference in ranking.

3.3 | Role of restrictions and socio-demographic, infrastructural and environmental factors

Next, we analyze potential associations between mortality and the socio-demographic, infrastructural, and environmental factors listed in Table 1. In doing so, we also consider two additional variables calculated from the mortality curves themselves, which we call *area before*, A_{bef} , and *area after*, A_{aft} . For each province, these measure the areas under the mortality curve to the left and the right, respectively, of the date when restrictions were introduced (March 9, 2020, for the first wave and November 4, 2021, for the second). Hence, they represent the cumulative mortality at the time of restriction and after restriction, respectively. As these variables are highly right-skewed, we take their logarithms to normalize them. Intuitively, before the introduction of restrictions the epidemic accelerates, with contagions spreading and, metaphorically, filling a pool of “potential deaths”. Restrictions, ideally, stop this process – or rather, in practice, curb it with varying degrees of effectiveness. After their introduction, as the mortality pattern unfolds over time, the pool of potential deaths empties. A_{bef} is our attempt at capturing how far the epidemic has accelerated before restrictions hit the breaks on it – and to do so based on mortality data, not cases, because data on the latter are so poor and unreliable. We use A_{bef} as a potential predictor in our regression models, along with socio-demographic, infrastructural, and environmental factors. In a way, it can be thought of as an “intermediate” predictor, subsuming the effects of a multitude of observed and unobserved factors, and influencing the subsequent unfolding of the mortality pattern. A_{aft} is our way to define a scalar summary of such pattern, capturing its cumulative severity. We use it as a simpler, scalar response – in alternative to the full mortality curve (functional response). A_{bef} is akin in spirit to other proxies used in recent studies to emphasize the importance of timely restriction policies in contrasting the spread of the epidemic. For example, using the first wave R_t and case data that are not publicly available, a recent study¹⁷ showed a strong relationship between the time spent above a given epidemic threshold prior to the introduction of restrictions and the total number of confirmed infections. Similarly, another recent study¹⁶ pinpointed the onset of the epidemic in an area and showed that the delay in such onset (and thus the shortening of the time between onset and restrictions) is a significant negative predictor of mortality levels.

To evaluate the relative importance of the factors considered in our study, we perform feature selection in two separate regression models. In the first, we use A_{aft} as scalar response, and implement an elastic net penalized fit³⁶ with the R package `glmnet`³⁷. In symbols, the corresponding minimization problem is

$$\min_{\beta} \left(\frac{1}{2} \|y - X\beta\|_2^2 + \lambda_1 \|\beta\|_1 + \frac{\lambda_2}{2} \|\beta\|_2^2 \right), \quad (2)$$

where n and p are the number of observations and features, respectively, $y \in \mathbb{R}^n$ is the response vector, $X \in \mathbb{R}^{n \times p}$ is the (standardized) design matrix, and $\beta \in \mathbb{R}^p$ is the coefficient vector. We set $\lambda_2 = 0.6\lambda_1$, and we run the fit for different values of λ_1 , starting from $\lambda_{max} = \|X^t y\|_{\infty}$, which selects 0 features, and gradually decreasing it. To capture the relevance of each feature, we track the λ_{max} -ratio for which it enters the model, defined as λ_{max} -ratio = $\lambda_j / \lambda_{max}$, where $\lambda_j \in (0, \lambda_{max})$ is the largest penalty weight such that feature j is included in the model; a higher ratio (earlier inclusion in the model) corresponds to higher relevance. Finally, to assess stability of the results, we repeat the procedure 500 times, each time using a random subset of \tilde{n} provinces, with \tilde{n} itself randomly selected between 90 and 107. By removing a random number of units randomly selected without replacement, we aim to mitigate the effect of potential outliers on our findings. In the second regression model, we use the full mortality curve as functional response, and employ `fgen`³⁸, which is an extension of the elastic net to settings where the response is functional. In this case, the minimization problem is

$$\min_{\beta_1(t), \dots, \beta_p(t)} \left(\frac{1}{2} \left\| y(t) - \sum_{j=1}^p X_j \beta_j(t) \right\|_{L^2}^2 + \lambda_1 \sum_{j=1}^p \|\beta_j(t)\|_{L^2} + \frac{\lambda_2}{2} \sum_{j=1}^p \|\beta_j(t)\|_{L^2}^2 \right), \quad (3)$$

where $y(t) = [y_1(t), \dots, y_n(t)]$ is the collection of n response curves, X is again the (standardized) scalar design matrix, $\beta(t) = [\beta_1(t), \dots, \beta_p(t)]$ is the collection of p coefficient curves, and $\|f\|_{L^2} = (\sum_{i=1}^n \|f_i\|_{L^2}^2)^{1/2}$ is the L^2 -norm for a generic function f . We handle λ_1 and λ_2 as in the scalar regression, track again the λ_{max} -ratio for each feature, and perform the same stability assessment repeating the procedure 500 times on random subsets of provinces. Results for both regressions, each fitted separately on first and second wave data, are summarized in the top graphics of Fig. 3A (elastic net for A_{aft}) and Fig. 3B (`fgen` functional elastic net for the mortality curves). Specifically, for each regression and wave, we display the features’ average λ_{max} -ratios across 500 runs on subsets of provinces. The predictor A_{bef} emerges as the most relevant by far in both regressions and in both

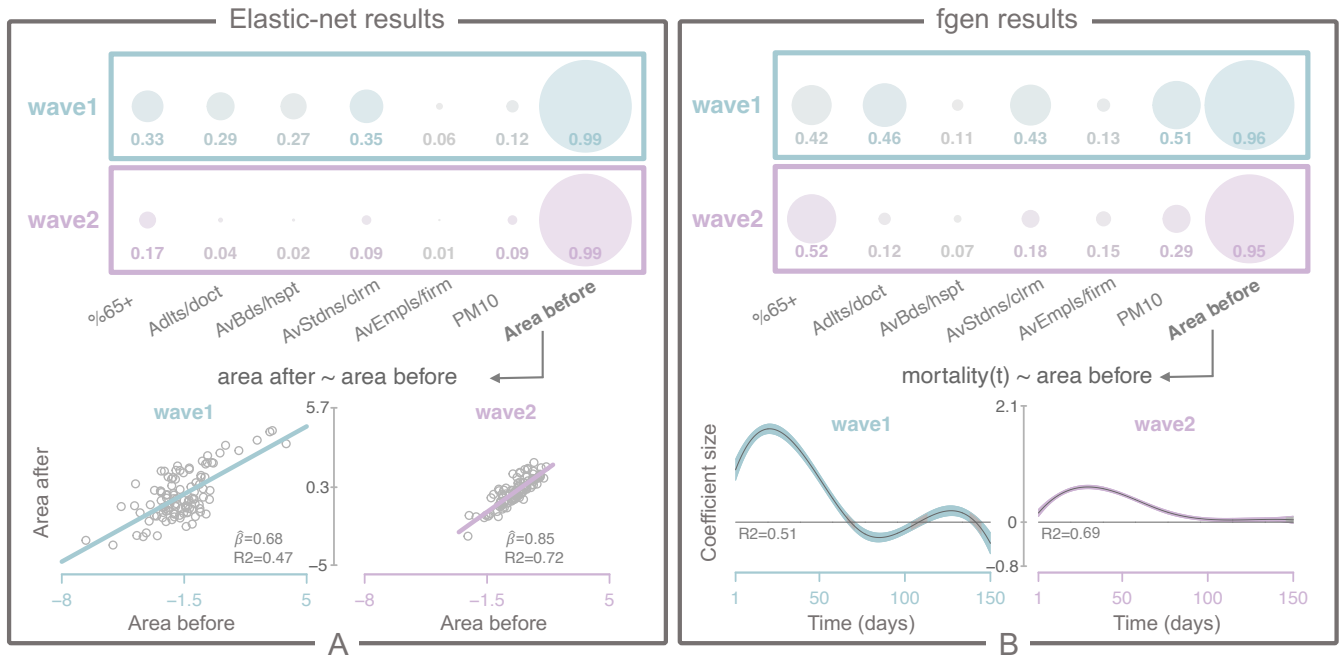


Figure 3 Feature selection results. Panel A: Elastic net results for A_{aft} (area after, scalar response). On the top, for each wave and each feature, we show balls with radius proportional to the average λ_{max} -ratio at which the feature enters the model across 500 replications of the regression on subsets of provinces (λ_{max} is the smallest penalty value associated with 0 selected features; the larger the λ_{max} -ratio, the earlier a feature is selected and the greater its relevance). On the bottom, for each wave, we show fitted line, coefficient estimate $\hat{\beta}$ and R^2 for the marginal regression of A_{aft} on A_{bef} (area before) – the most relevant feature in both waves – run an all 107 provinces (marginal regression results for other predictors are provided in Fig. S5). Panel B: Functional elastic net (fgen) results for mortality curves, in a format similar to Panel A. For the marginal regressions of mortality curves on A_{bef} , bottom plots show coefficient curve estimates $\hat{\beta}(t)$ as black solid lines, with bands built adding and subtracting $1.96\times$ point-wise standard errors (marginal regression results for other predictors are provided in Fig S6).

waves, with the largest average λ_{max} -ratios. Table S1 and Figure S4 report results of the elastic net and fgen feature selections obtained on the full data set comprising all the 107 provinces and with the parameter λ_1 chosen by 5-fold cross-validation.

As a parallel exercise, for each response and wave, we run marginal regressions on every predictor separately – using the full set of 107 provinces. Results concerning A_{bef} are shown in the bottom graphics of Figs. 3A and 3B. Specifically, we display scatter plots with fitted lines, coefficient estimates and R^2 s for the marginal regressions of A_{aft} on A_{bef} in first and second wave, and coefficient curve estimates and R^2 s for the marginal functional regressions of mortality curves on A_{bef} , again in first and second wave. Marginal results are consistent with the elastic net feature selection, confirming strong positive (i.e. aggravating) statistical effects of A_{bef} on both waves of the epidemic. In particular, A_{bef} has the largest marginal R^2 's among all predictors considered; results concerning all other predictors are provided in Fig. S5 (A_{aft}) and in Fig S6 (mortality curves).

The primacy of A_{bef} in our analyses provides further evidence that the timing of restrictions may play a crucial role in modulating the epidemic. Comparing marginal and joint results between the two waves, its effect appears to be larger in magnitude in the second wave for the scalar response, and in the first wave for the functional response. The R^2 's are always larger in the second wave though, likely due to the fact that then both A_{aft} and the mortality curves exhibited less variability. In addition to being generally weaker, the roles of socio-demographic, infrastructural, and environmental factors appear to vary depending on the response, as well as the wave. For instance, considering mortality curves, adults per family doctor and average students per classroom exhibit a strong signal in the first wave, along with $PM10$ – confirming previous findings³. However, the relevance of these predictors decreases in the second wave, where the percentage of inhabitants over 65 seems to play a stronger role. These differences may result in part from the existence of collinearity among features (see Figs. S7 and S8), with the variable A_{bef} possibly subsuming a number of other effects, but they may also reflect actual changes that occurred between the two waves. For instance, average students per classroom (as measured in 2019; see Table 1) may indeed have been a good proxy for the ability

of schools to act as contagion hubs during the first wave, but may have become a much less meaningful predictor during the second wave – when classroom sizes were reduced, many activities were held online, and even when attending school in person students had to adhere to masking and social distancing protocols.

Finally, we compute $pc1$ – the first principal component of the socio-demographic, infrastructural, and environmental factors in Table 1, which can be used as an overall summary to control for their effects (A_{bef} is not included in this computation). $pc1$, which explains 65.6% of the overall variance, is mainly driven by adults per family doctor and average beds per hospital (see loadings in Fig. S5B), and presents only a very mild correlation with A_{bef} (see Fig. S9C). We therefore further gauge the role of A_{bef} by running both the scalar regressions (with response A_{afi}) and the functional regressions (with response the mortality curves) using A_{bef} and $pc1$ as joint predictors, and computing their *partial* R^2 s. Results from these joint fits (see Fig. S9) support our previous statements, highlighting once again the importance of A_{bef} . As a reminder, the partial R^2 of a predictor is defined as $(R^2 - R_{red}^2)/(1 - R_{red}^2)$, where R^2 is the coefficient of determination of the complete model, and R_{red}^2 that of the model comprising all predictors but the one being evaluated.

3.4 | Mobility patterns

Several studies^{7,39,40} found evidence that local, short-range mobility worked as a key modulator of COVID-19 spread. We therefore produce province-level mobility curves based on Google’s “Grocery & Pharmacy” and “Workplace” indexes – which express percentage changes in mobility linked to these categories with respect to a pre-pandemic reference (the first five weeks of 2020; see Section 2.3). Before analyzing how mortality relates to local mobility (see Section 3.5 below), we compare patterns in the latter between the two waves, highlighting some marked differences. During the first wave, local mobility showed a dramatic reduction with respect to reference values, suggesting that the restrictions implemented by the government were generally effective in changing people’s behaviors. In more detail, the mobility curves in Fig. 4A show the “Grocery & Pharmacy” index reaching levels between -50% and -60% (depending on the province) during the first wave lockdown. This reduction occurred even though citizens were allowed to leave their homes for these necessities. In the same period, and in particular after the halting of all non-essential production activities on March 23, 2020, the “Workplace” index reached even lower levels, dipping to values between -60% and -80% . In contrast, during the second wave, while local mobility still contracted with respect to the reference, reductions were less dramatic. The “Grocery & Pharmacy” curves reached minima between 0% and -20% . Those of the “Workplace” index again dipped deeper, between -40% and -60% , but only around Christmas and New Year – when the entire country was red-coded to try and take advantage of the holidays to curb the second epidemic wave. Also strikingly, the variance across curves was very low during the first wave, and much higher during the second.

In summary, mobility decreased dramatically and uniformly across the country during the first wave lockdown, and only moderately, with more variability from province to province – likely as a consequence of the adaptive restrictions imposed by the color-coded system – during the second wave. Notably, these patterns did not just reflect differences in the severity and uniformity of the restrictions themselves, but also differences in citizens’ attitudes. While during the first wave people limited also activities that were permitted by the lockdown rules, during the second wave they took fuller advantage of whatever mobility was allowed to them.

3.5 | Association between mobility and mortality

We now turn to the analysis of the association between mobility and mortality curves. To begin, we attempt to evaluate the delay between changes in the former and their potential impact on the latter. For each province in each wave, we compute a *lag*, defined as the number of days elapsed between the date in which mobility restrictions were introduced and the date in which the province experienced its mortality peak. Restricting attention to the provinces which did experience a discernible epidemic in each wave (those in the hard- and medium-hit clusters 2 and 3; see Section 3.2), Fig. 4B shows a scatterplot of peak values against lags, together with their marginal distributions, for the two waves. For these provinces, lags are much more spread in the second wave than in the first, but their medians are remarkably similar (19 and 17 days, respectively). In contrast, peak values are higher and much more spread in the first wave than in the second; in particular, the first wave peak distribution has a long right tail. Notably, there appears to be a distinct negative relationship between lag and peak size in the first wave, which provides yet more evidence for the importance of restrictions timing. In the provinces most severely affected by the epidemic, restrictions came too late to curb mortality; these provinces reached their very high mortality peaks shortly after the implementation of the national lockdown. In contrast, provinces that, while affected, were spared the worst impacts were those where restrictions came

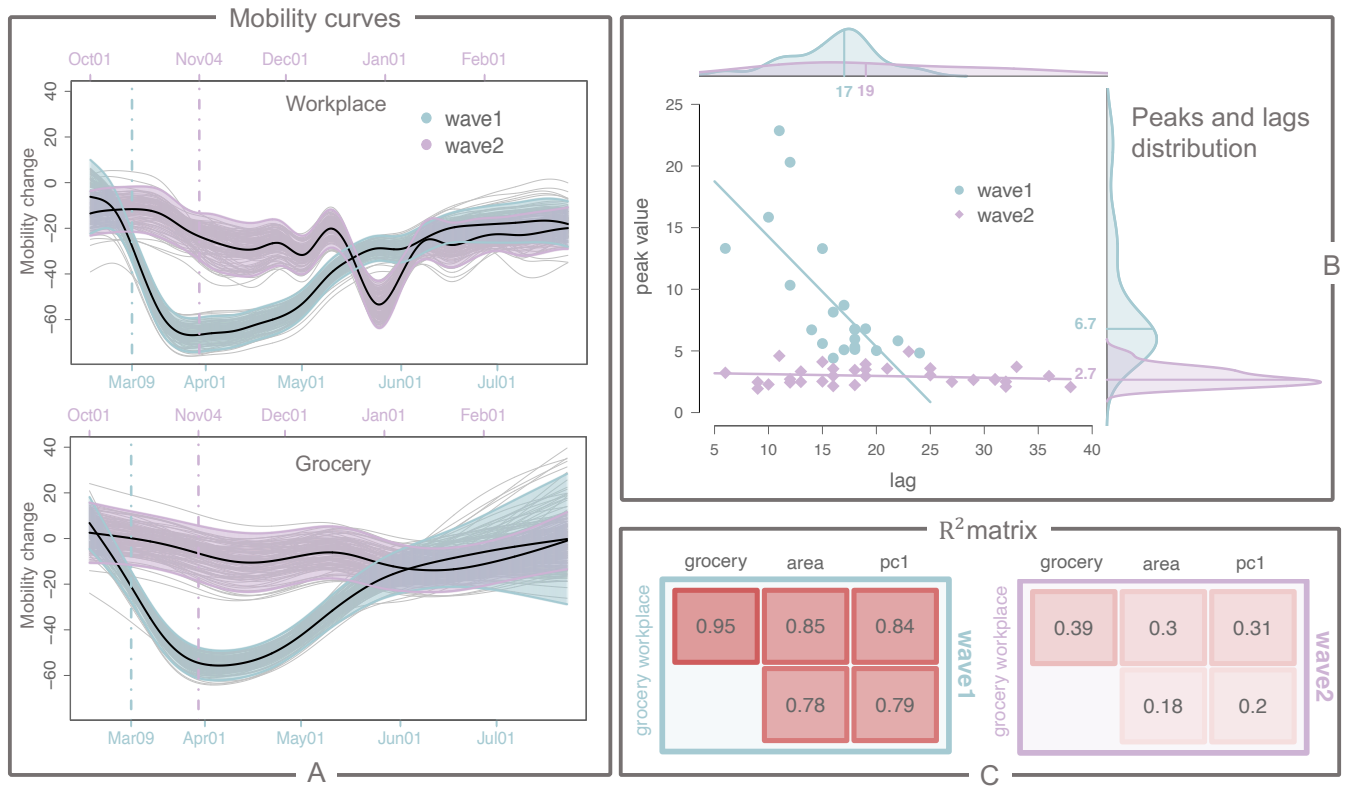


Figure 4 Mobility and lags. Panel A: “Grocery & Pharmacy” and “Workplace” mobility curves during first and second wave. Solid black lines are functional means, with bands built by adding and subtracting $1.96\times$ point-wise standard deviations. Vertical lines mark dates when mobility restrictions were introduced (March 9, 2020, and November 4, 2020, for first and second wave, respectively). Panel B: scatterplot and marginal distributions of peak values and lags for provinces with a discernible epidemic (hard- and medium-hit clusters 2 and 3; see Section 3.2) in first and second wave. Lags are defined as the number of days between the mobility restriction date and the mortality peak for each province. Least-squares regression lines on the scatterplot have negative estimated slopes of -0.89 (significant) for the first wave and -0.01 (non-significant) for the second. Vertical lines on the marginal distributions mark medians. Panel C: R^2 values, obtained by regressing each functional variable in the rows against each functional and scalar variable in the columns, in first and second wave. These are used to gauge predictor collinearities prior to modeling mobility curves. Background color intensity in each block is proportional to the R^2 .

earlier during the epidemic progression; they had smaller peaks occurring at a later stage. Intriguingly, an analogous negative relationship between lags and peaks cannot be traced in the second wave, when even in the worst-hit provinces peak values remained relatively low.

Next, we attempt to evaluate the impact of mobility on mortality developing appropriate regression models. We consider as potential predictors of mortality curves both “Grocery & Pharmacy” and “Workplace” mobility curves, as well as two scalar variables from our prior analyses; A_{bef} (which summarizes the progression of mortality up to the introduction of restrictions), and $pc1$ (which summarizes the factors listed in Table 1). To gauge collinearities, we fit functional regressions of “Grocery & Pharmacy” and “Workplace” on each other, and on each of the scalar variables. Fig. 4C shows the resulting R^2 s which, together with the correlations reported in Figs. S8 and S9C, provide an overall picture of the dependence structure among explanatory variables. In the first wave, predictors show very strong linear associations. In particular, “Grocery & Pharmacy” and “Workplace” mobility exhibit an R^2 of 0.95, confirming the effectiveness of the first lockdown. Both mobility indices are also highly correlated with A_{bef} (the R^2 is 0.78 for “Grocery & Pharmacy” and 0.85 for “Workplace”). A possible explanation is that, while mobility plummeted everywhere, whatever variation existed in such reduction across the country saw places hardest hit by the epidemic up to the lockdown date contract mobility the most. Because of these strong associations, to avoid variance inflation phenomena, we consider a very simple model for the first wave (Model A) – regressing mortality curves only on one type of mobility curves, say “Workplace”, and $pc1$ as a control variable. In the second wave, predictors show much milder linear

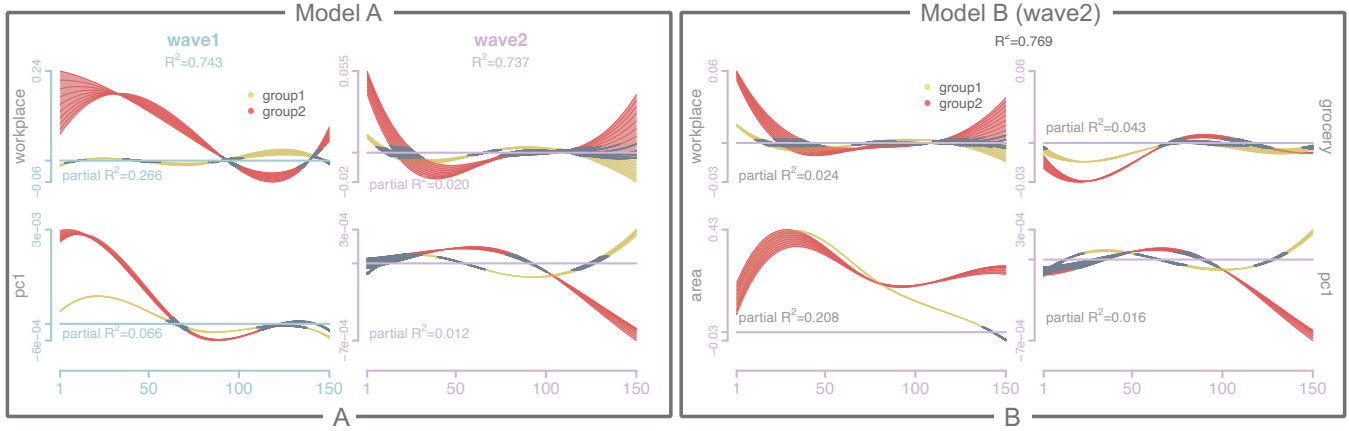


Figure 5 Lagged concurrent functional regression results. Panel A: for first (left) and second (right) wave, estimated coefficient curves for the regression of mortality on “Workplace” mobility and *pc1*, with an additional binary predictor separating provinces with mild ($d = 0$, Group 1) vs. hard/intermediate ($d = 1$, Group 2) epidemic courses. The plots show “beams” comprising 10 curves, one for each of the lags considered in the model ($\ell = 15, \dots, 24$). Gray portions in a curve correspond to time intervals where it did not significantly depart from 0 (the confidence interval obtained adding and subtracting to the estimate $1.96\times$ pointwise standard errors contained 0). For each regression we report the average total and partial R^2 's over the 10 fits with different lags. Panel B: in a format similar to A, but for the second wave only, results for the regression of mortality on “Workplace” mobility, “Grocery & Pharmacy” mobility, A_{bef} and *pc1*, again including the binary predictor separating provinces with mild vs. hard/intermediate epidemic courses.

associations. The more nuanced and differentiated color-coded restrictions allowed “Grocery & Pharmacy” and “Workplace” mobility to vary more across the country and to capture different signals, with an R^2 decreasing to 0.39. Also the R^2 's with A_{bef} decrease (to 0.18 for “Grocery & Pharmacy” and 0.30 for “Workplace”). We therefore consider both the simple model used for the first wave (Model A), and a more complex model (Model B) – regressing mortality curves jointly on both types of mobility curves, A_{bef} and again *pc1* as a control.

In both Model A and Model B we also introduce a binary predictor d to separate provinces with discernible epidemics (hard- and medium-hit clusters in Section 3.2; $d = 1$, Group 2) from the others (mild-cluster; $d = 0$, Group 1). Finally, we formulate both models as “lagged” concurrent function-on-function regressions^{2,41}. The functional response (mortality) at time t is thus assumed to depend only on a functional predictor (mobility) at time $t - \ell$, where ℓ (the lag) is an additional model parameter. In symbols, the general formulation we utilize is

$$y(t) = \alpha(t) + \alpha_d(t)d + \sum_{m=1}^M \left(\beta_m(t - \ell)X_m(t - \ell) + d\beta_{m,d}(t - \ell)X_m(t - \ell) \right) + \sum_{j=1}^J \left(\beta_j(t)X_j + d\beta_{j,d}(t)X_j \right) + \epsilon(t), \quad (4)$$

where, as before, $y(t) = [y_1(t), \dots, y_n(t)]$ is the collection of n shifted mortality curves, $n = 107$, and $\epsilon(t)$ are i.i.d. Gaussian errors. M is the number of functional predictors ($M = 1$ in Model A and $M = 2$ in Model B), all introduced with the same lag ℓ , and J is the number of scalar covariates ($J = 1$ in Model A and $J = 2$ in Model B). Finally, $\alpha(t)$, $\beta_m(t - \ell)$, and $\beta_j(t - \ell)$ are functional intercept and coefficient curves for provinces where the epidemic was mild ($d = 0$) while $\alpha(t) + \alpha_d(t)$, $\beta_m(t - \ell) + \beta_{m,d}(t - \ell)$, and $\beta_j(t) + \beta_{j,d}(t)$ are the corresponding curves for provinces where the epidemic was hard/intermediate ($d = 1$). Before fitting our models, we shift mobility curves by applying, for each province, the same shift used to align mortality curves (Fig. S10 shows the mobility curves after shifting). Moreover, based on the distributions of lags reported in Fig. 4 and on previous findings⁴², we fit the models with 10 different values of ℓ ranging from 15 to 24 days – note that this range includes the medians of the lag distributions for both waves. Estimating coefficient curves at different lags addresses potential stability pitfalls in modeling functional objects and provides a more robust understanding of the relationship between the investigated variables⁴³. Indeed, testing various lags allows us to determine whether the estimated functional coefficients are heavily influenced by the specific lag, or whether they exhibit a consistent effect that is not contingent on the specific value of ℓ within the range considered. To fit functional regressions we use the R package `refund`⁴⁴, which estimates functional coefficients and their standard errors.

Fig. 5A summarizes results for Model A fitted (separately) on both waves. As expected, coefficient curve estimates are generally larger in magnitude for the first vs. the second wave, and for hard/intermediate hit vs. mildly hit provinces. In both waves, “Workplace” mobility is the leading predictor variable (based on the partial- R^2). Its effect is positive along most of the domain during the first wave, but only at the beginning of the second wave. Notably, coefficient curve estimates are fairly consistent in shape and magnitude across lags in the 15-to-24 day range, suggesting stability of our findings. Robustness to varying model specifications is also confirmed using “Workplace” mobility and the group dummy d as predictors (without $pc1$ as control; see Fig S11B), or replacing “Workplace” with “Grocery & Pharmacy” mobility (with $pc1$ and d ; see Fig. S11A, or without $pc1$; see Fig S11B). Interestingly though, coefficient curve estimates for “Grocery & Pharmacy” are slightly negative in the first half of the second wave. A mild (and temporary) negative association between this type of mobility and mortality may in fact make sense; there was not a hard policy restriction against these first necessity-type of movements, and the public may have engaged in them more liberally in provinces with lower mortality and a perception of (relative) safety. Finally, Fig. 5B summarizes results for Model B fitted on the second wave. Coefficient curve estimates for both mobility predictors (“Grocery & Pharmacy” and “Workplace”), which are here considered jointly, are consistent with those obtained from fits of Model A. However, the predictor with the largest partial R^2 here is A_{bef} , which shows a strong positive association with mortality – providing yet more evidence for the critical role of restriction timing. Interestingly, the effect size of A_{bef} is similar in hard/intermediate and mildly hit provinces during the first half of the period covered by the second wave. This may be due to the definition of A_{bef} , which is the integral of the curve in the first part of the domain (before restrictions take place). As in Model A, coefficient curve estimates are consistent in shape and magnitude across lags in the 15-to-24 day range, indicating a strong and stable effect. Furthermore, total and partial R^2 s are comparable across lags. Thus, both the explanatory power of the model and the relationships between response and predictors are stable across the range of lags considered, lending reliability to our findings.

4 | DISCUSSION

Notwithstanding the limited availability and at times poor quality of publicly available data, we were able to leverage techniques from the domain of functional data analysis to characterize and compare the initial two waves of the COVID-19 pandemic in Italy. Our analysis is conducted at the provincial level; this finer resolution compared to prior studies by our group and others^{3,45,46,47} allowed us to shed additional light on critical associations and relationships – avoiding the loss of signal caused by spatial aggregations and enabling the use of more sophisticated statistical models. The two waves span a complete year, from February 2020 to February 2021, and both occurred before the beginning of the vaccination campaign. Therefore, the patterns and associations we observed were not influenced by vaccine availability and the progressive increase of vaccine-related immunity in the country.

Using hierarchical clustering, we identified three clusters in both waves of the pandemic; one representing a mild mortality pattern, and two representing an intermediate strength and a harsh exponential pattern, respectively. Perhaps the most interesting observation obtained by contrasting clustering results for the two waves is that some of the provinces most impacted during the first wave (e.g., Bergamo, Como, and Lodi in Lombardia) were among the least impacted during the second. This could have been due to a reduced number of vulnerable individuals after the deaths in the first wave, to behavioral adaptations that led the population in these areas to adhere more strictly to recommendations on, e.g., social distancing and mask use, and possibly to a degree of herd immunity.

Next, we highlighted the importance of a timely introduction of restrictions. Given the poor quality of data on cases, we created a variable, A_{bef} , that quantifies the escalation of the epidemic prior to the introduction of restrictions based on mortality data alone. Using a number of regression analyses and techniques we found A_{bef} to be a very strong predictor of mortality in both waves – in fact a stronger and more consistent predictor than the proxies for socio-demographic, infrastructural, and environmental factors at our disposal. Potentially suboptimal proxies, collinearity, and possible confounding effects require that we interpret these results with care. But they do suggest that, by “hitting the breaks” on the exponential dynamics of mortality, restrictions play a pivotal role in curbing the spread of the epidemic and mitigating its impact.

Finally, we explored the relationships between mortality and mobility patterns. During the first wave lockdown, mobility exhibited very pronounced and similar contractions across the country. Following the introduction of the second wave color-coded restriction system, mobility contractions were milder and more geographically differentiated. Despite these differences, through additional functional regression exercises we were able to identify significant and robust positive associations between mobility and mortality in both waves.

This study, alongside our previous work³, demonstrates the potential of functional data analysis techniques for analyzing epidemiological data. We note that, while some of the techniques employed here are well-established, others are relatively recent and provided new and valuable insights.

ACKNOWLEDGMENTS

M.A. Cremona acknowledges the support of the Natural Sciences and Engineering Research Council of Canada (NSERC), of the Fonds de recherche du Québec Health (FRQS), and of the Faculty of Business Administration, Université Laval. F. Chiaromonte acknowledges support from the Huck Institutes of the Life Sciences, Penn State.

Author contributions

All authors conceived ideas and analysis approaches. T.B., J.Di I., and L.T. retrieved and processed data from multiple public sources, implemented pipelines, and performed statistical analyses. All authors interpreted findings and participated in the writing of the manuscript. M.A.C. and F.C. supervised the research.

Data availability

Data for replication are available at <https://github.com/tobiaboschi/fdaCOVID2>.

References

1. Kokoszka P, Reimherr M. *Introduction to functional data analysis*. CRC Press . 2017.
2. Ramsay JO, Silverman BW. *Functional data analysis*. Springer. 2 ed. 2005.
3. Boschi T, Di Iorio J, Testa L, Cremona MA, Chiaromonte F. Functional data analysis characterizes the shapes of the first COVID-19 epidemic wave in Italy. *Scientific reports* 2021; 11(17054): 1–15.
4. Collazos JA, Dias R, Medeiros MC. Modeling the evolution of deaths from infectious diseases with functional data models: The case of COVID-19 in Brazil. *Statistics in Medicine* 2023; 42: 993-1012.
5. Engle S, Stromme J, Zhou A. Staying at home: mobility effects of COVID-19. *Available at SSRN 3565703* 2020: 1–16.
6. Nepomuceno MR, Acosta E, Alburez-Gutierrez D, Aburto JM, Gagnon A, Turra CM. Besides population age structure, health and other demographic factors can contribute to understanding the COVID-19 burden. *Proceedings of the National Academy of Sciences* 2020; 117(25): 13881–13883.
7. Nouvellet P, Bhatia S, Cori A, et al. Reduction in mobility and COVID-19 transmission. *Nature communications* 2021; 12(1): 1–9.
8. Hastie T, Tibshirani R, Friedman J. *The elements of statistical learning: data mining, inference, and prediction*. Springer Science & Business Media . 2009.
9. Ciminelli G, Garcia-Mandicó S. COVID-19 in Italy: an analysis of death registry data. *Journal of Public Health* 2020; 42(4): 723–730.
10. Henry NJ, Elagali A, Nguyen M, Chipeta MG, Moore CE. Variation in excess all-cause mortality by age, sex, and province during the first wave of the COVID-19 pandemic in Italy. *Scientific reports* 2022; 12(1): 1–12.
11. Buoro S, Di Marco F, Rizzi M, et al. Papa Giovanni XXIII Bergamo Hospital at the time of the COVID-19 outbreak: letter from the warfront. *J Lab Hematol*. 2020; 42: 8–10.
12. Senni M. COVID-19 experience in Bergamo, Italy. *Eur Heart J*. 2020.

13. Golinelli D, Lenzi J, Adja K, et al. Small-scale spatial analysis shows the specular distribution of excess mortality between the first and second wave of the COVID-19 pandemic in Italy. *Public Health* 2021; 194: 182–184.
14. Perico N, Faggioli S, Di Marco F, et al. Bergamo and COVID-19: how the dark can turn to light. *Frontiers in medicine* 2021; 8: 609440.
15. Vinceti M, Filippini T, Rothman KJ, Di Federico S, Orsini N. The association between first and second wave COVID-19 mortality in Italy. *BMC Public Health* 2021; 21(1): 1–9.
16. Basellini U, Camarda CG. Explaining regional differences in mortality during the first wave of COVID-19 in Italy. *Population Studies* 2021; 76: 1–20.
17. Cintia P, Pappalardo L, Rinzivillo S, et al. The relationship between human mobility and viral transmissibility during the COVID-19 epidemics in Italy. *arXiv preprint* 2020; arXiv:2006.03141: 1–37.
18. Craven P, Wahba G. Smoothing noisy data with spline functions. *Numerische mathematik* 1978; 31(4): 377–403.
19. Ramsay JO, Wickham H, Graves S, Hooker G. *fda: Functional Data Analysis. R package version 2.2-6* 2011.
20. DPC . COVID-19 dati-province. <https://github.com/pcm-dpc/COVID-19/tree/master/dati-province>; 2020.
21. DPC . COVID-19 dati-regioni. <https://github.com/pcm-dpc/COVID-19/tree/master/dati-regioni>; 2020.
22. Arpino B, Bordone V, Pasqualini M. No clear association emerges between intergenerational relationships and COVID-19 fatality rates from macro-level analyses. *Proceedings of the National Academy of Sciences* 2020; 117(32): 19116–19121.
23. ISTAT . Popolazione residente al 1° gennaio in tutti i comuni. <http://dati.istat.it/Index.aspx>; 2020.
24. ISTAT . Atlante Statistico dei Comuni. <http://asc.istat.it/ASC/>; 2020.
25. Ministry of Health . Open Data. <https://www.dati.salute.gov.it/dati/dettaglioDataset.jsp?menu=dati&idPag=18>; 2021.
26. Ministry of Education . Portale unico dei dati della scuola. <https://dati.istruzione.it/opendata/opendata/catalogo/#Scuola>; 2021.
27. Stekhoven DJ, Bühlmann P. MissForest: non-parametric missing value imputation for mixed-type data. *Bioinformatics* 2012; 28(1): 112–118.
28. ISTAT . Tavole dati: Ambiente urbano. <https://www.istat.it/it/archivio/236912>; 2020.
29. Google . Community mobility reports. <https://www.google.com/covid19/mobility/>; 2021.
30. Modi C, Böhm V, Ferraro S, Stein G, Seljak U. Estimating COVID-19 mortality in Italy early in the COVID-19 pandemic. *Nature communications* 2021; 12(1): 1–9.
31. Borghesi A, Golemi S, Carapella N, Zigliani A, Farina D, Maroldi R. Lombardy, Northern Italy: COVID-19 second wave less severe and deadly than the first? A preliminary investigation. *Infectious Diseases* 2021; 53(5): 370–375.
32. Chirico F, Nucera G, Szarpak L. COVID-19 mortality in Italy: The first wave was more severe and deadly, but only in Lombardy region. *Journal of Infection* 2021; 83(1): e16.
33. Zirilli A, Limonti F, Alibrandi A. COVID-19 Pandemic Waves in Italy: An Epidemiological Overview about Infections, Swabs and Death Rates. *Open Journal of Epidemiology* 2022; 12(3): 285–299.
34. Hartigan JA. *Clustering algorithms*. John Wiley & Sons, Inc. . 1975.
35. Randolph HE, Barreiro LB. Herd immunity: understanding COVID-19. *Immunity* 2020; 52(5): 737–741.
36. Zou H, Hastie T. Regularization and variable selection via the elastic net. *Journal of the royal statistical society: series B (statistical methodology)* 2005; 67(2): 301–320.

37. Friedman J, Hastie T, Tibshirani R, Narasimhan B. glmnet. *R package version 4.1-3* 2021.
38. Boschi T, Reimherr M, Chiaromonte F. A Highly-Efficient Group Elastic Net Algorithm with an Application to Function-On-Scalar Regression. *Advances in Neural Information Processing Systems* 2021; 34: 9264–9277.
39. Cuéllar L, Torres I, Romero-Severson E, et al. Assessing the impact of human mobility to predict regional excess death in Ecuador. *Scientific reports* 2022; 12(1): 1–12.
40. Rahman MM, Thill JC. Associations between COVID-19 Pandemic, Lockdown Measures and Human Mobility: Longitudinal Evidence from 86 Countries. *International Journal of Environmental Research and Public Health* 2022; 19(12): 7317.
41. Horváth L, Kokoszka P. *Inference for functional data with applications*. 200. Springer Science & Business Media . 2012.
42. Cartenì A, Di Francesco L, Henke I, Marino TV, Falanga A. The role of public transport during the second COVID-19 wave in Italy. *Sustainability* 2021; 13(21): 11905.
43. Yu B, Kumbier K. Veridical data science. *Proceedings of the National Academy of Sciences* 2020; 117(8): 3920–3929.
44. Goldsmith J, Scheipl F, Huang L, et al. refund: Regression with functional data. *R package version 0.1-16* 2016.
45. Azzolina D, Lorenzoni G, Silvestri L, Prosepe I, Berchiolla P, Gregori D. Regional differences in mortality rates during the COVID-19 epidemic in Italy. *Disaster Medicine and Public Health Preparedness* 2022; 16(4): 1355–1361.
46. Della Rossa F, Salzano D, Di Meglio A, et al. A network model of Italy shows that intermittent regional strategies can alleviate the COVID-19 epidemic. *Nature communications* 2020; 11(1): 5106.
47. Guzzi PH, Tradigo G, Veltri P. Spatio-temporal resource mapping for intensive care units at regional level for COVID-19 emergency in Italy. *International journal of environmental research and public health* 2020; 17(10): 3344.

SUPPLEMENTARY MATERIAL

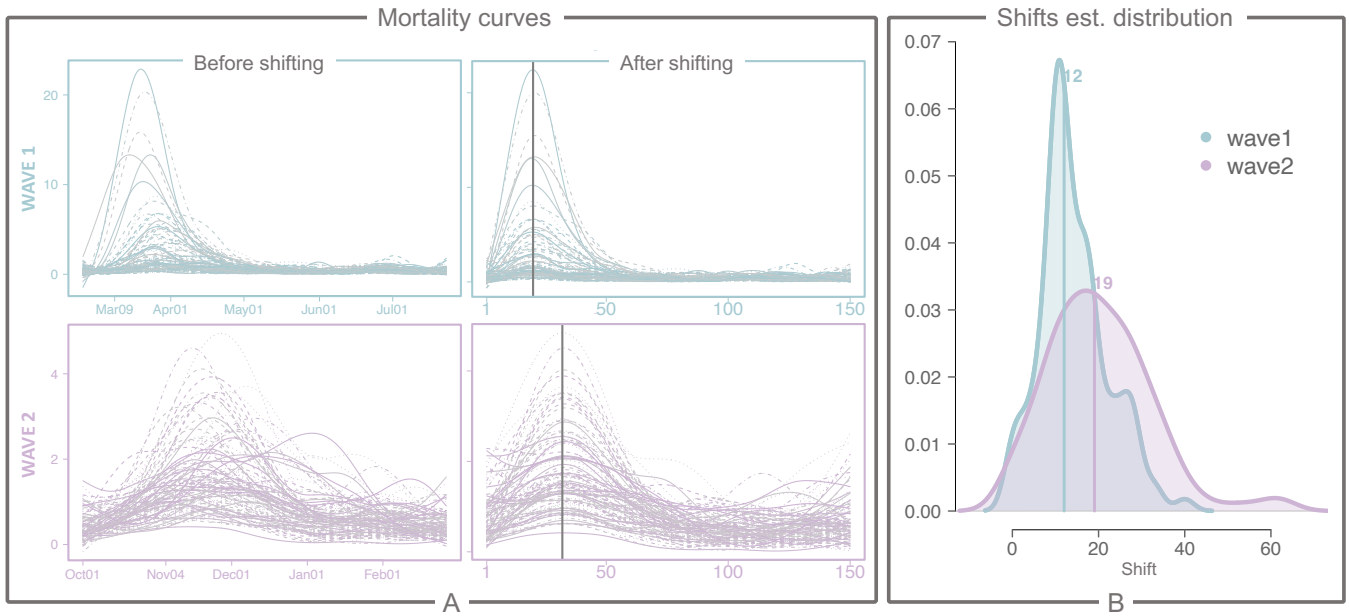


Figure S1 Mortality before and after alignment. Panel **A** represents the mortality curves in the first (top) and second (bottom) wave, before (left) and after (right) the shifting to align their peaks. The vertical line on the shifted curves indicates the new common peak time, which has been set to be equal to the time of the earliest peak – day 20 (peak of Lodi) for the first wave and day 33 (peak of Cagliari) for the second wave. Panel **B** represents the distributions of the estimated shifts in the two waves. The vertical lines at 12 and 19, respectively, are the median of the two distributions.

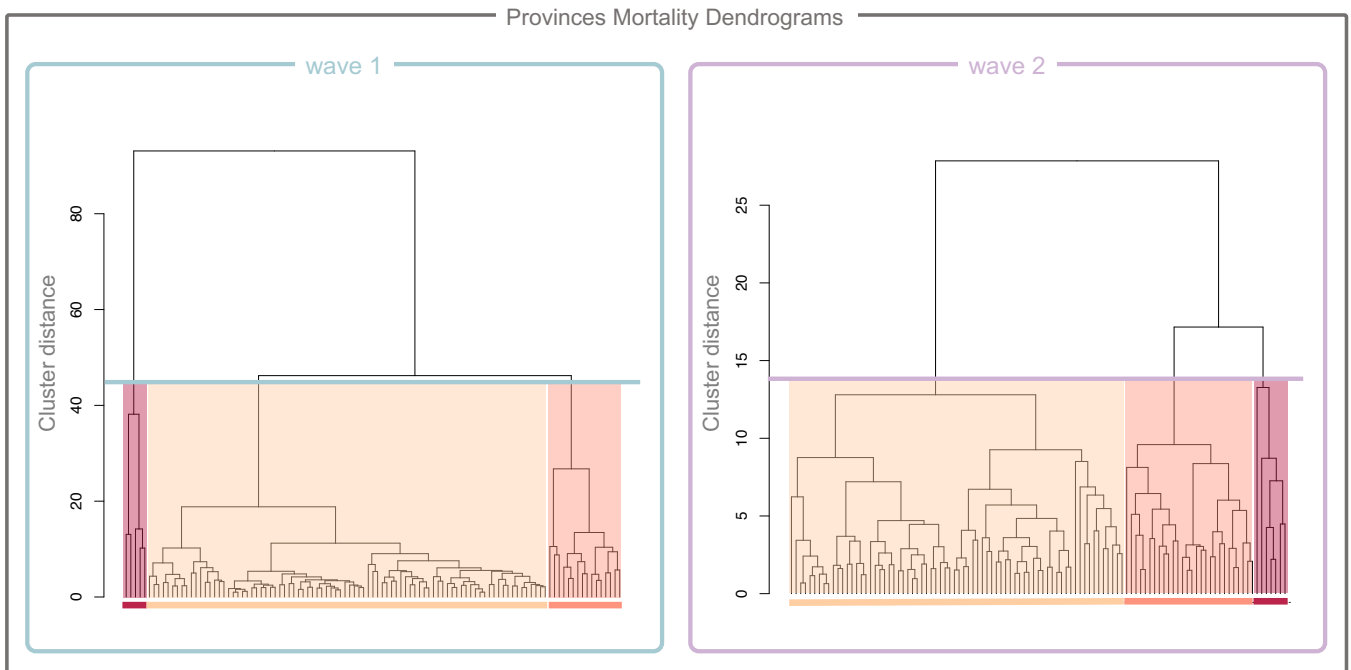


Figure S2 Provinces mortality dendrograms. The figure displays the dendrograms for both waves, obtained using agglomerative clustering with L^2 distance and complete linkage. Note that the vertical axes, representing the distances between clusters, have different scales for the two waves – implying that clusters in wave 2 are less distinct than the ones in wave 1.

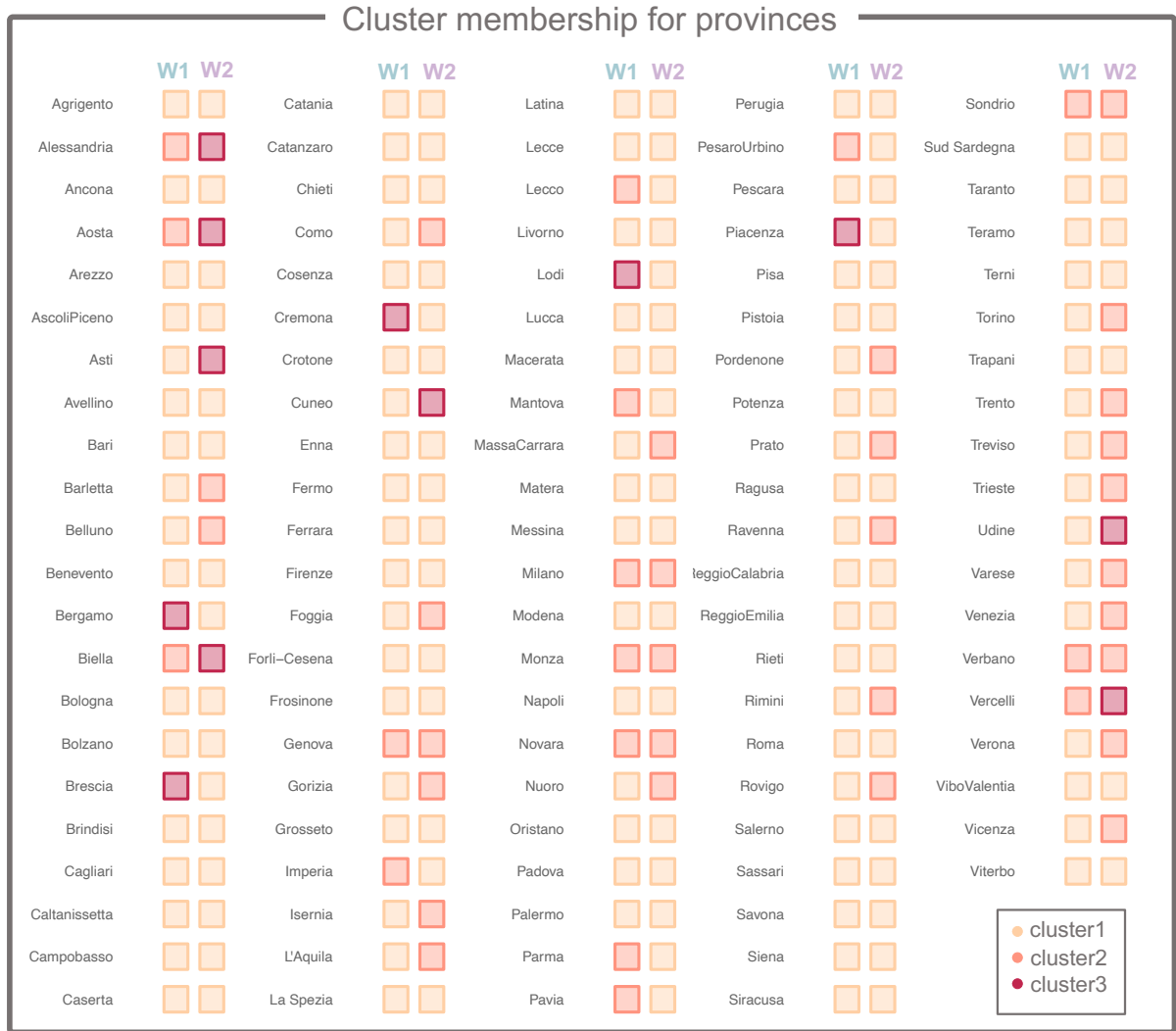


Figure S3 Cluster membership for provinces. Cluster membership of each province in the first and in the second wave (W1 and W2, respectively).

Table S1 Joint elastic net fit. Elastic net coefficients corresponding to optimally chosen λ_1 via 5-fold cross-validation (we set $\lambda_2 = 0.6\lambda_1$). For each wave, we show the results corresponding to the minimum cross-validation error (λ_1^{min}) as well as the ones at one standard deviation of the minimum (λ_1^{1se}). Models are fitted on the full data set comprising all 107 provinces. All variables are standardized. Dots imply that the associated variable has not been selected by the model (coefficient equal to 0).

Variable	Wave 1		Wave 2	
	$\lambda_1^{min} = 0.0036$	$\lambda_1^{1se} = 0.0978$	$\lambda_1^{min} = 0.0344$	$\lambda_1^{1se} = 0.1293$
Over 65	0.2079	0.1001	0.0776	0.0106
Adults per family doctor	0.0615	0.0369	0.0035	.
Ave. beds per hospital	0.0778	0.0493	.	.
Ave. students per classroom	0.1565	0.1037	0.0211	.
Ave. employees per firm	0.0595	.	.	.
PM10	0.0670	.	0.0567	.
Area before	0.6049	0.5178	0.7810	0.6649

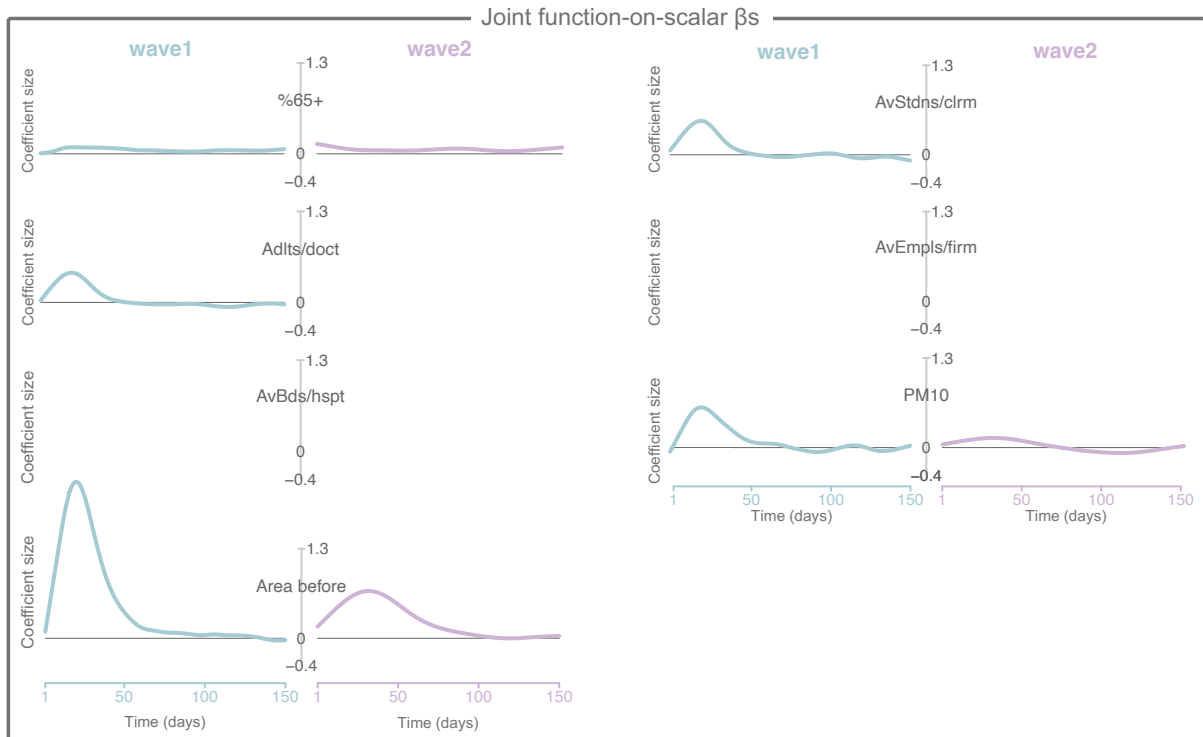


Figure S4 Joint function-on-scalar fit. fgen functional coefficients corresponding to optimally chosen λ_1 via 5-fold cross-validation (we set $\lambda_2 = 0.6\lambda_1$). Models are fitted on the full data set comprising all 107 provinces. All variables are standardized. Empty plots imply that the associated variable has not been selected by the model (coefficient equal to 0).

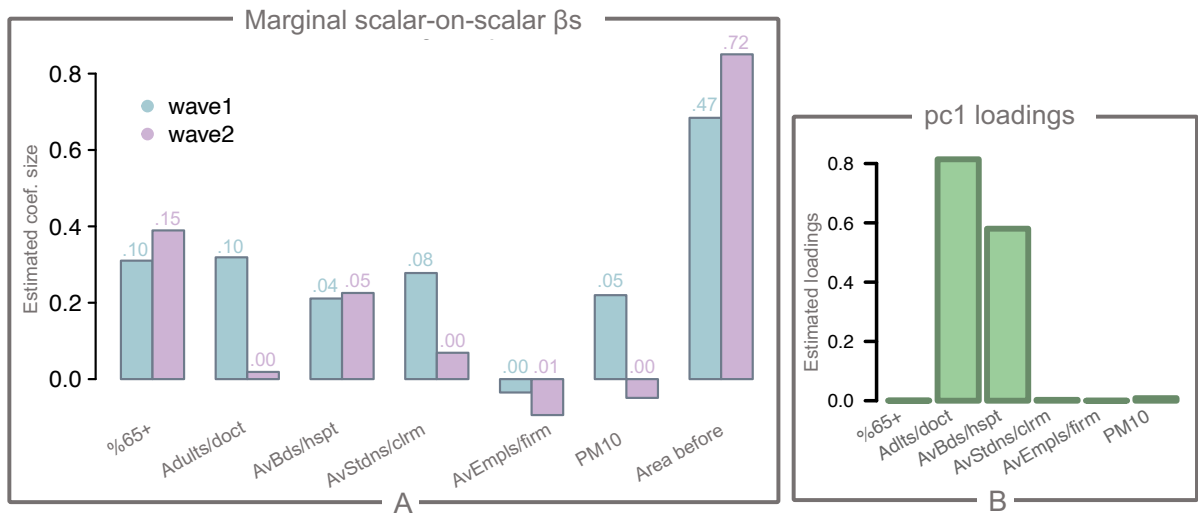


Figure S5 Marginal scalar-on-scalar results. Panel A shows the estimated coefficients $\hat{\beta}$ for the marginal regression of A_{aft} (area after, scalar response) on individual scalar features. The associated marginal R^2 is reported above each coefficient bar. Panel B shows the loadings of the first principal component computed considering all the scalar features but A_{bef} (which explains 65.6% of the variance).

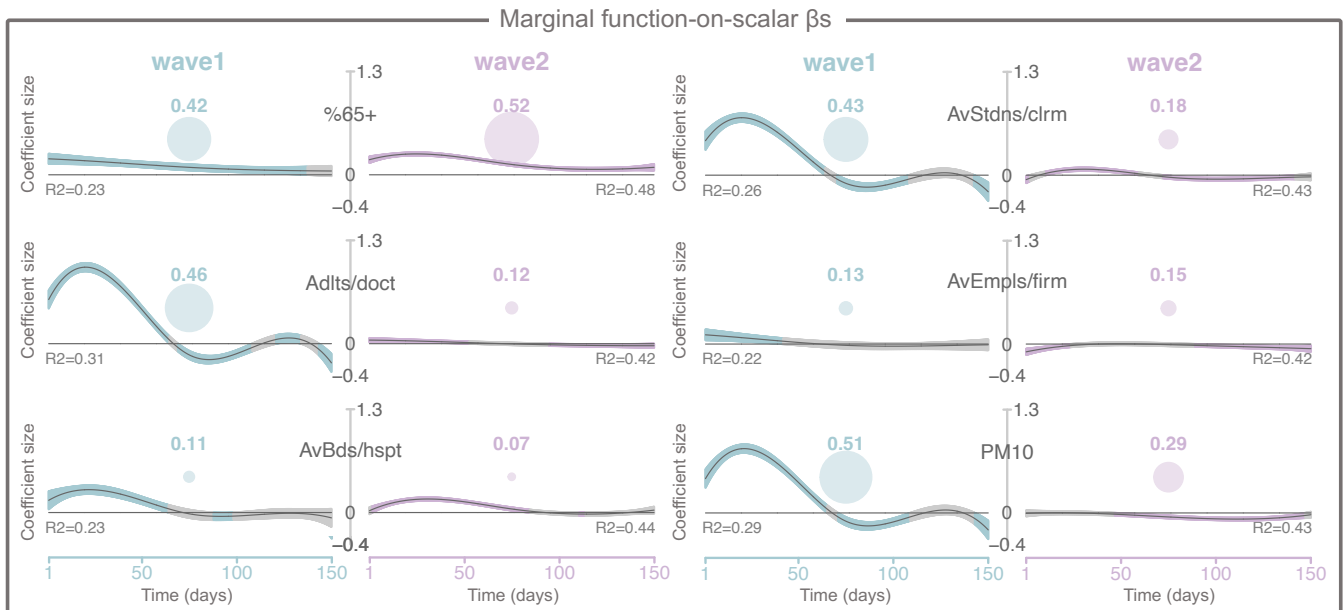


Figure S6 Marginal function-on-scalar results. The figure depicts the estimated coefficient curves $\hat{\beta}(t)$ for the marginal regression of the mortality curve on individual scalar covariates. The black solid lines represent $\hat{\beta}(t)$, with bands built adding and subtracting $1.96\times$ pointwise standard errors. Grey areas denote the parts of the time domain where the bands contain the value 0. For each regression, we report its R^2 as well as the λ_{max} -ratio for which the variable enters in the fgen feature selection model (balls are proportional to λ_{max} -ratio).

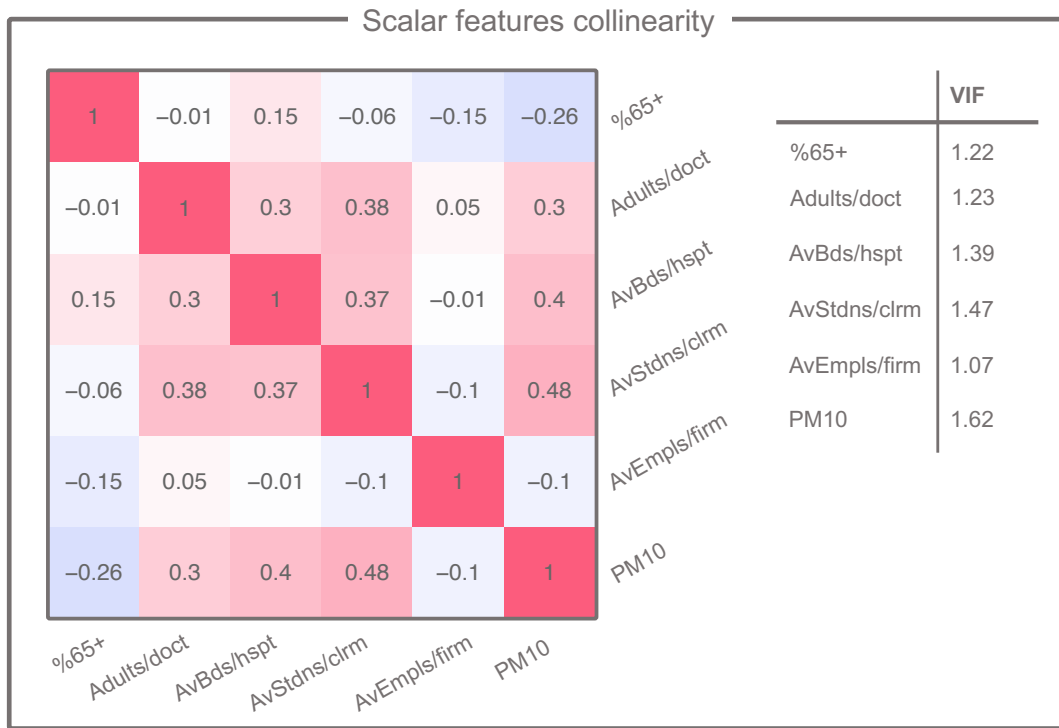


Figure S8 Scalar feature collinearity. The matrix on the left displays the pairwise correlation between the six scalar features employed in the main analysis. The table on the right contains their variance inflation factors (VIF).

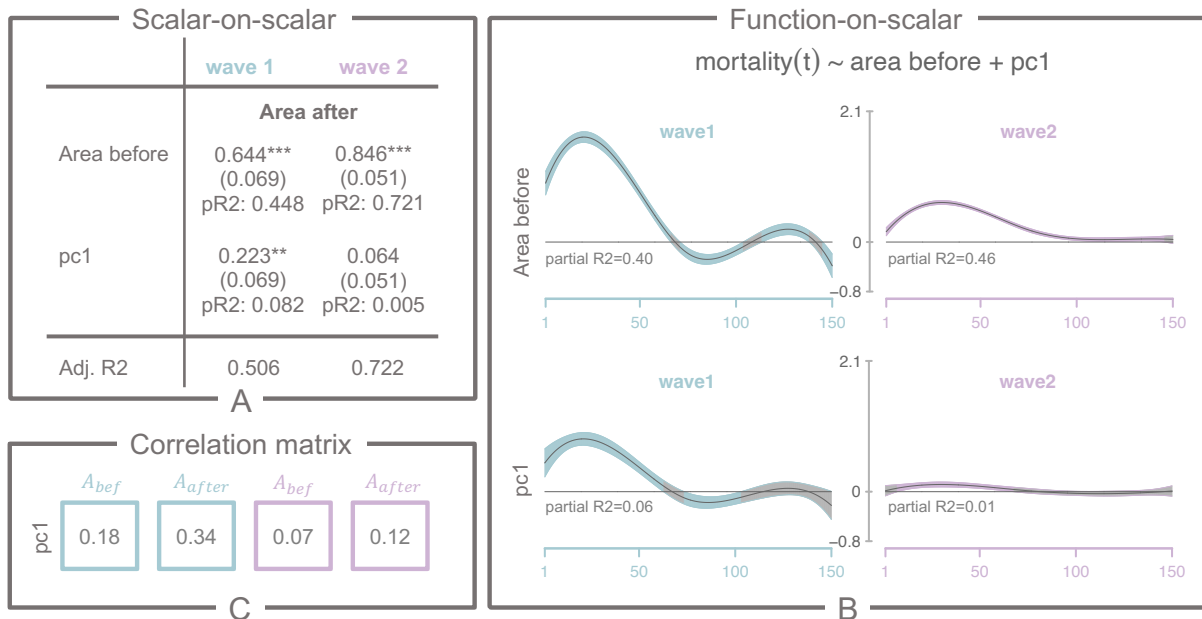


Figure S9 Joint effects of area before and $pc1$. Panel A shows the results of the joint regression of A_{aft} on A_{bef} and $pc1$. For both waves and for each variable, we show the estimated coefficient (with significance indicated by stars), its standard error in parenthesis, and the associated partial R^2 . Clearly, area before dominates $pc1$ in terms of explanatory power. Panel B depicts the estimated coefficients curves $\hat{\beta}(t)$ for the joint regression of mortality on the scalar covariates area before and $pc1$. The black solid line represents the estimated mean, with bands built adding and subtracting $1.96\times$ pointwise standard errors. Grey areas denote the parts of the time domain where the bands contain the value 0. For each regressor, we report the corresponding partial R^2 . Panel C shows, for each wave, the correlation between $pc1$ and A_{bef} and A_{after} .

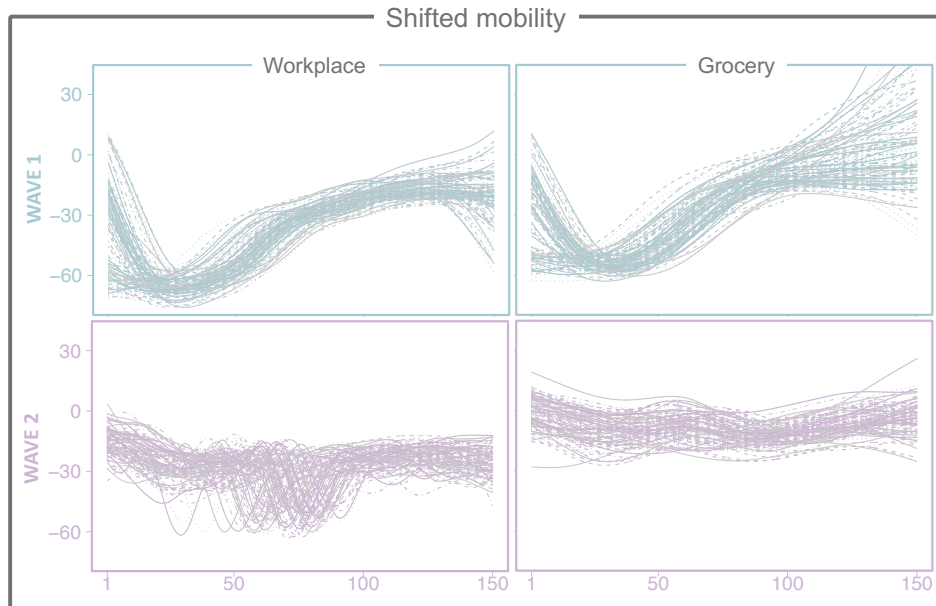


Figure S10 Shifted mobility. The figure depicts "Workplace" and "Grocery & Pharmacy" mobility after we apply the shifts estimated on the mortality curves.

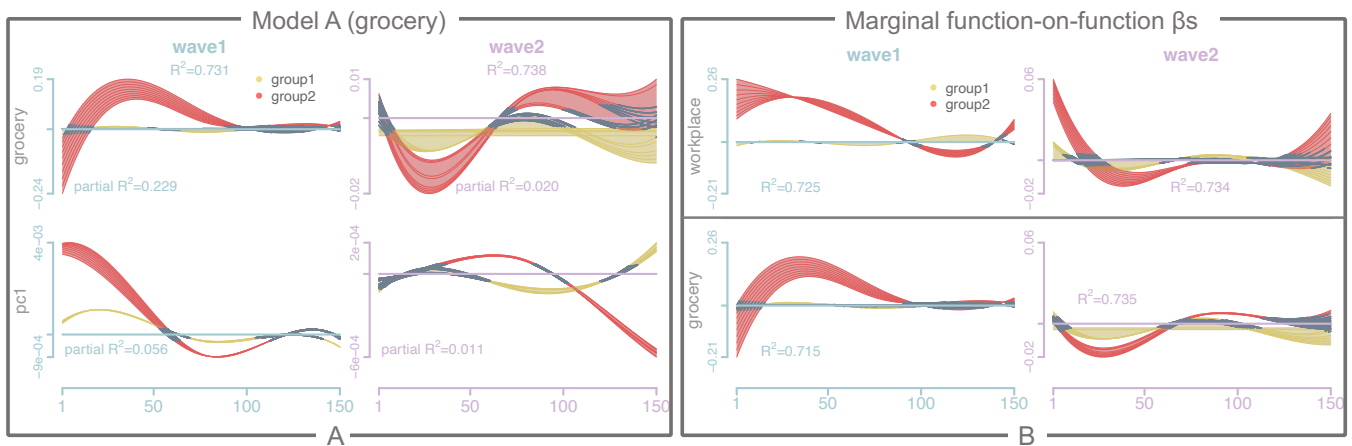


Figure S11 Lagged concurrent functional regression results. Panel A shows, for both waves, the estimated coefficient curves for the regression of mortality on "Grocery & Pharmacy" mobility and *pc1*, with an additional binary predictor separating provinces with mild ($d = 0$, Group 1) vs. hard/intermediate ($d = 1$, Group 2) epidemic courses. The plots show "beams" comprising 10 curves, one for each of the lags considered in the model ($\ell = 15, \dots, 24$). Gray portions in a curve correspond to time intervals where it did not significantly depart from 0 (the confidence interval obtained adding and subtracting to the estimate $1.96 \times$ pointwise standard errors contained 0). For each regression, we report the average total and partial R^2 's over the 10 fits with different lags. Panel B shows, in a format similar to A, results for the marginal regression of mortality on mobility curves.